Analytical Methods

A Luminescent Nanocrystal Metal Organic Framework for Chemosensing of Nitro Group Containing Organophosphate Pesticides

Journal:	*Analytical Methods*
Manuscript ID:	AY-ART-12-2013-042189.R4
Article Type:	Paper
Date Submitted by the Author:	08-Apr-2014
Complete List of Authors:	KUMAR, PAWAN; CSIR-CSIO, Chandigarh, Nano Sciences & Technology; CSIR-CSIO, Chandigarh, Nano Sciences & Technology Paul, A.; CSIR-CSIO, Chandigarh, Nano Science and Nano Technology (H-1), Deep, Akash; CSIR-CSIO, Chandigarh, Nano Sciences & Technology

A Luminescent Nanocrystal Metal Organic Framework for Chemosensing of Nitro Group Containing Organophosphate Pesticides

Pawan Kumar[$#*], A.K. Paul[$#], Akash Deep[$#]

[$]Central Scientific Instruments Organisation (CSIR-CSIO), Sector 30 C, Chandigarh, 160030, India

[#]Academy of Scientific and Innovative Research, CSIR-CSIO, Sector 30 C, Chandigarh, 160030, India

*Tel: 0172-2657811 (452-Ext), Fax: 0172-2657287,

Email: pawannano10@gmail.com,dr.akashdeep@csio.res.in

Abstract. A luminescent nanocrystal metal–organic framework (NMOF**1**) of [Cd(atc)(H_2O)$_2$n] has been synthesized by the reaction of Cd(II) ions with the sodium salt of H_2atc (2-aminoterephthalic acid) in aqueous solution. The obtained fluorescent porous material has been characterized by X-ray diffraction, transmission electron microscopy, confocal microscopy, UV-Vis spectroscopy, photoluminescence spectroscopy and surface area analysis. The synthesized NMOF**1** exhibits reasonably good fluorescence characteristics (excitation wavelength = 340nm, emission wavelength = 436 nm). The potential of above Cd(II) based nanocrystal metal–organic framework (NMOF**1**) for the sensing of nitro aromatic containing organophosphate pesticides (OPs) parathion, methyl parathion, paraoxon and fenitrothion is demonstrated. It has been possible to detect the above four OPs separately in the concentration range of 1ppb - 500 ppb. The detection limit of the proposed method for all the said OPs is 1ppb. Interestingly, their mixture also shows the above characteristic data. The proposed method for the sensing of nitroaromatic OPs is also selective towards other OPs such as malathion, dichlorvos and monocrotophos.

Keywords: Nanocrystal Metal Organic Framework, Chemosensening, Nitroaromatic Compound, Organophosphate Pesticides.

Introduction

Organophosphates pesticide (OPs) compounds are highly toxic and affect the neural system of the organism, which may lead to several lethal problems to human beings and may cause neurological disorders [1-2]. These compounds disposal in the open environment is regulated and their routine monitoring is important for maintaining desired standards of water resources and food supplies [3-4]. Various OPs e.g. parathion, methyl parathion, paraoxon and fenitrothion are widely used products by the agriculture industry which have nitroaromatic compounds. Parathion is one of the most toxic and widely used insecticides. It converts to paraoxon and leaves residues on plant surfaces [5]. The resulting residues persist in the environment and present hazards especially in hot and dry agricultural areas, where the agricultural products are not properly washed before storage. The toxicity due to parathion is known to affect animal life and is responsible for many illnesses and deaths [6]. Fenitrothion is also one of the most hazardous and broad spectrum insecticide used for pest control in rice, vegetables, wheat, cereals, and cotton. Though fenitrothion has low mammalian toxicity, it is known to disrupt endocrine [7].

Many analytical methods are available for the detection of OPs, including gas chromatography (GC), high-performance liquid chromatography (HPLC) and mass spectroscopy [10]. Most of these methods are very sensitive and reliable, but the requirements of large set-ups, expensive instrumentation and highly skilled manpower requirement limit their applicability. Currently, enzymatic biosensors have been explored as viable, handy and portable alternative with fair levels of sensitivity and accuracy [11]. The sensitive biosensors based on acetylcholinesterase (AChE) / butyryl cholinesterase (BChE) inhibition, or organophosphate hydrolase (OPH) induced hydrolysis have been developed for the monitoring of OPs [12] . The limitation of the immunoassays method involves the requirements of label process [13]. A label-free electrochemical immunosensor with paraoxon antibodies

loaded on the gold nanoparticles has been reported for the monitoring of paraoxon in aqueous samples, but it has poor selectivity and specificity [14]. Recently, solid phase extraction (SPE) of OPs combined with square-wave voltammetric analysis, and electrochemical sensing with zirconia nanoparticles-decorated graphene hybrid nanosheets have been highlighted for convenient and cost-effective enzyme-less sensing [15-17]. A highly sensitive fluorescent chemosensor for fenitrothion has been reported using per-6-amino-β-cyclodextrin:Eu(III) complex [18]. The sensor system showed sensitivity response in the order, fenitrothion > quinalphos > methylparathion > parathion > methylparaoxon > paraoxon > fenchlorphos > profenofos >malathion. The comparison studies really important and very help to assess the environmental quality, protection of water resources, food supplies, and monitoring of the detoxification processes.

Recently, the luminescent MOFs have been found new and interesting applications in the sensing of small molecules, solvents and explosives [19-20]. The detectable changes in luminescence of MOFs by tuning the host–guest chemistry along with the tunable porosity and high surface area makes MOFs the excellent candidates in sensing applications. The pioneering work of Wang et al.[22] sparked research activities towards exploiting the potential of luminescent MOFs in explosives detection and small molecules sensing [23-24]. However the bulky MOFs have limited interaction between MOFs and analytes in solvent, lower solubility nature in well known solvents [25-26]. In other hand, nanocrystal metal–organic frameworks (NMOFs) attracted due to better dispersive nature which makes them easily contact with small molecules with no loss in their intrigue framework architectures and topologies. In addition, high luminescence of NMOFs provides opportunity to implement them for the development of unique sensing materials [28-30]. Basically, NMOFs are new class of hybrid materials built from metal ions with well- defined coordination geometry and organic bridging ligands and already explored a number of promising and potential applications in

catalysis, nonlinear optics, and small molecules sensing [31-32]. However, capability of NMOF**s** for the solid phase extraction of pesticides has not been proposed by some other researchers. Conjugated NMOF**s** with high dimensionality may also be beneficial as sorbents for the solid phase extraction of nitroaromatic OPs by direct physical adsorption. The mixing of OPs with NMOF is characterized with synergetic effects of weak interactions (e.g. hydrogen bond) and π----π stacking. In light of the above discussion, MOFs may be envisaged as very useful compounds for the simultaneous extraction and sensing of OPs in different environmental samples.

The present work explores the utility of a luminescent NMOF**1** for the direct chemosensing of nitro OPs, including parathion, methyl parathion, paraoxon and fenitrothion. The $Cd(atc)(H_2O)_2n$ (ATC : 2-aminoterephthalic acid) has been synthesized via coprecipitation method. The synthesized product has been characterized with help of different instrumental techniques. The NMOF**1** was incubated with different concentrations of nitro aromatic OPs and the change in the fluorescence intensity recorded which may due to strong electron withdrawing $–NO_2$ group. The electrostatic interaction between the photoexcited $Cd(atc)(H_2O)_2n$ and electron withdrawing $–NO_2$ moiety has led to a pesticide concentration dependent change in the fluorescence intensity. In addition, the proposed method is also selective with respect to malathion, dichlorvos and monocrotophos due to absence of $–NO_2$ moiety.

Experimental Section

Materials. $Cd(NO_3)_2$, 2-aminoterephthalic acid, distilled water, parathion, methyl parathion, paraoxon,fenitrothion, malathion, dichlorvos and monocrotophoswere high purity grade chemicals from Sigma-Aldrich / Merck / Fisher Scientific. All other chemicals and solvents were A.R / G.R grade products from Sigma-Aldrich.

Synthesis of NMOF**1.** 1.10ml of 0.05M Cd $(NO_3)_2$ and 10ml of 0.5M of sodium salt of H_2atc (2-aminoterephthalic acid) were taken in aqueous solution. A large amount of white precipitate was generated immediately. After vigorous stirring of one hour at room temperature precipitate was collected by centrifugation and washed with water and ethanol (2 x10ml). For the NMOF**1** photoluminescence (PL) and pesticide sensing experiments, the ethanolic suspensions of NMOF**1** (2mg/mL) were prepared by sonication for 5 min. The homogenous suspensions were transferred in 1 mm optical cells for further measurements.

Characterization/ equipment. X-ray Diffraction (XRD, Shimadzu 6000), Field-Emission Scanning Electron Microscopy coupled with Energy Dispersive X-ray Spectroscopy (FE-SEM – EDX, Hitachi 4300/SN), Confocal Laser Scanning Microscopy (CLSM, Zeiss LSM 510) and Transmission Electron Microscopy (TEM, Hitachi H-7500) were used to confirm the crystal phase, lattice pattern and morphology of the prepared MOF-5 particles.Nitrogen isotherm analysis was done with Micromeritics ASAP- 2020 sorptometer. Thermal stability was tested using a thermogravimetric analyzer (TGA, SDT Q600 thermal gravimeter). UV-visible absorption and photoluminescence spectra were measured by UV-visible-NIR spectrophotometer (Varian Cary 5000) and PL spectrophotometer (Varian). Fourier transform infrared (FTIR) spectra were recorded on a Nicolet iS10 spectrophotometer equipped with an attenuated total reflectance (ATR) accessory.

Nitro OPs sensing. Stock solution of the nitro OPs (parathion, methylparathion, paraoxon, fenitrothion) was diluted / prepared in ethanol. Known diluted volumes of the stock solutions were prepared and mixed with the ethanolic suspension of NMOF**1** (2 mg/mL). The contents were thoroughly mixed and then incubated at 25^0C for 5 min. The PL intensity of the reaction mixture was measured and correlated with OPs concentration. The selectivity experiments with respect to malathion, dichlorvos and monocrotophos were also carried out in similar fashion.

All the above experiments were done in triplicate and the average data value have been reported.

Results and Discussion

X-ray Diffraction Analysis. Wang et al. [33] have reported powder PXRD measurement for crystal structure and chemical composition of bulky [Cd(atc)$(H_2O)_2$n]. Thus NMOF**1** has monoclinic crystal structure with space group C_2/C. The sodium salt of H_2atc and self-assembling of Cd(II) ions may be attributed to formation of NMOF**1** architectures. The Cd (II) ion is six coordinated with a greatly distorted octahedral geometry and consists of 1D zigzag motifs with non-covalent interactions. These 1D zigzag motifs chain leads to formation of 3D network structure. The PXRD [Fig. 1 (**I)**] peak positions of the herein synthesized NMOF**1** product matches with the reported NMOF**1** materials [Fig. 1 (**II)**] [33, 34]. The sharpness and high intensity indicate high crystallinity of the NMOF**1**, which is also supported by FESEM data [Fig. 1 (**I)**]. The NMOF**1** is stable and easily dispersed in common solvent ethanol, benzene, and nitrobenzene. The peak at 19.6^0 is reasonably high, and corresponds to the reflections of octahedral geometry structure.

Fig.1 [**a & b]** shows the FE-SEM images of the synthesized NMOF**1** samples. FE-SEM scanning at a comparatively lower magnification to cover large sample area indicates towards the formation of nanocrystals. Higher resolution FE-SEM imaging suggests the formation of single phase octahedral crystals Fig.1 (**b).** Nanocrystals was also evidenced in the FE-SEM investigations; however, we could also obtain some scans of isolated octahedral crystals. Typical diameter of the product was estimated to be around 100 – 500 nm.

To study the thermal stability of NMOF**1** [34-36], the thermo gravimetric analysis (TGA) was performed under a nitrogen atmosphere in presence of N_2 gas with a heating rate of 10 ^{0}C min $^{-1}$ in the temperature range 25–900 ^{0}C. The TGA curve of the NMOF**1** is divided into two stages where the first weight loss 19.1% occurs in the temperature range 41–265 ^{0}C, which

can be attributed to the loss of both lattice structure and coordinated water molecules (calculated value 19.6%). Subsequent, there is an individual weight loss stage in the temperature range of 311–497 ^{0}C, corresponding to the loss of the organic ligand due to the formation of CdO. The residual weight of 34.9% may correspond to the final product of CdO (calculated value 36.1%).

The FTIR spectrum (Fig. 2) of the synthesized NMOF**1** has been characteristics bands of 1610, 1507, 1570, 1457 and 1358 cm^{-1}. The fundamental vibrations have assigned to stretching vibrations at higher energy and bending vibrations at lower energy of C-O in carboxylate groups respectively [34]. The bands at 3500 – 3200 cm^{-1} accounts for the adsorbed water.

The excitation and emission spectra of NMOF**1** are already reported in literature [33, 34]. In our study, a strong blue emission at around 436 nm was observed by excitation at 349 nm for [Cd (atc) $(H_2O)]_n$ in ethanol. The observed blue emission which can be assigned to the luminescence from intra-ligand emission excited state [34]. The emission from [Cd (atc) $(H_2O)]_n$ primarily originates from surface defects, such as ionizable oxygen vacancies or cd (II) ions vacancies on the surface. Broad absorption and emission spectra of in NMOF**1** crystals suggests that the transition responsible for the photoluminescence takes place between deeply trapped charges (localized donor and acceptor levels). Most of the defects in the NMOF**I** crystals exist inside.

The above studies have verified the synthesis of porous NMOF**1** crystals with their particle size in the range of 100 – 500 nm. The blue emission of these NMOF**1** crystals and their porous structures has further been utilized for convenient, label free and sensitive chemosensing of $–NO_2$ group containing OPs.

Chemosensing of $–NO_2$ OPs. Fig. 1(**C**) shows the photoluminescence spectra of NMOF**1** in the presence of different concentrations (1 ppb – 1 ppm) of parathion. Methyl parathion,

paraoxon and fenitrothion also exhibited similar effect on the PL of NMOF**1**.Their data are not shown in order to avoid repeatability. There is a loss observed in the NMOF**1** photoluminescence (PL) upon interaction with the above OPs solutions. The concentration of the pesticides plays an important role in deciding the degree of PL quenching. Interestingly, all the four tested OPs quench the PL of NMOF**1** to similar degree. Consequently, a mixture of all the above four pesticides was prepared having equal fractions to prepare 1 ppb – 1 ppm solutions. The mixing of this mixture of nitro OPs with NMOF**1** also resulted in to the quenching of PL [Fig. 1(**D**)]. In all the above cases, a linear trend was observed from 1 ppb – 500 ppb concentration. The detection limit of the sensing was 1 ppb, below which the changes in the NMOF**1** PL were miniscule and unstable. The stability and reproducibility of the measurements was checked by recording the change of PL intensity of different sets of NMOF**1** suspensions (2 mg/mL) in the presence of 1 ppb, 5 ppb, 100 ppb and 500 ppb nitro OPs mixture. The results are shown in different sets of NMOF**1** provided similar degrees of PL quenching and their measurements were stable for a minimum of 48hr.

The selectivity of the above sensing of nitro OPs with NMOF**1** with respect to some other OPs such as malathion, dichlorvos and monocrotophos was also investigated [Fig. 3(**a & b**)]. A 10 ppb mixture of nitro OPs was incubated with NMOF**1** suspension in the presence of 10 and 100 fold concentration (100 ppb and 1 ppm) of malathion, dichlorvos and monocrotophos. Similarly, the test was also undertaken in the combined presence of 1 ppm of malathion, dichlorvos and monocrotophos. In both the investigations, the degree of PL quenching corresponded to the presence of 500 ppb of nitro OPs. Separate experiments only with the solutions of malathion, dichlorvos and monocrotophos suggested no significant of PL quenching which is due to absence of strong electron withdrawing group [Fig. 3 (**b**)].

The dominant mechanism of luminescence attenuation of NMOF**1** in the presence of nitro aromatic OPs can be attributed to the interactions of the analytes with the ligand molecule.

NMOF**1** generates a valence band hole (h_{VB}^{+}) and a conduction band electron (e_{CB}-) during the band gap excitation. These photogenerated (h_{tr}^{+}) or trapped (e_{tr}^{-}) carriers participate in the redox processes with the nitro OPs at the surface or inside the NMOF**1** particle. The quenching of NMOF**1** emission can be analyzed by considering equilibrium between the uncomplexed and complexed NMOF**1** particles with the analyte moieties. It may be assumed that the quenching of NMOF**1** emission occurs only in the associated complex between NMOF**1** and nitro OPs; and therefore, the association constant K_a may be given as

$$I_0/(I_0 - I) = I_0/(I_0 - I') + I_0/\{K_a \times (I_0 - I') \times [OP]\} \qquad \text{eq [1]}$$

Where I_0 is the initial emission intensity of the NMOF**1** particle, I is the emission intensity after adding the OP of concentration *[OP]* and *I'* is the emission intensity of the OP used. Fig. 4 shows the straight-line plot of $I_0/(I_0 - I)$vs.*1/[OP]*, which confirms the validity of the equilibrium model. The K_a values for various nitroaromatic OPs are computed and given in Fig 5. Stern-Volmer relationship has been utilized to assess the quantitative characteristics of the PL quenching process. These experiments have been conducted using the PL quenching data with various concentrations of the OPs. Stern-Volmer constant (K_{SV}) can be calculated according to the following equation

$$(I_0/I) - 1 = K_{SV}\,[OP] \qquad \text{eq [2]}$$

A plot of I_0/Ivs. *[OP]* gives progressive linear relationship for all the nitro OPs, whereas saturation behaviour was observed in case of malathion, dichlorvos and monocrotophos (Fig. 6). Since $K_{SV} = k_q^{av}\,\tau_0$; the average quenching rate constant k_q^{av} can also be computed keeping the value of τ_0(lifetime of NMOF**1** PL) as 0.66 µs [36]. In the different PL quenching experiments with nitro OPs, the k_q^{av}values (Fig. 6) are comparable or higher than the typical diffusion-controlled rate constants, $\sim 10^{10} M^{-1}s^{-1}$ in the bulk solution [36]. These parameters confirm the diffusion of the nitro OPs molecules on to the surface as well in to the porous

structure of the NMOF**1**. The diffusion process may be correlated with the level of detection sensitivity offered by the NMOF**1**. The computed k_q^{av} values (Fig. 6) for malathion, dichlorvos and monocrotophos are indicative of the non-diffusion process and absence of nitro group or strong electron withdrawing group, which might be linked with the inability of these OPs to quench the PL of NMOF**1**. The different k_q^{av} values may also be correlated with the oxidation potential E_{ox} of the related OPs. The E_{ox} values of parathion (-0.02 V), methyl parathion (0.05 V), paraoxon (0.5 V) and fenitrothion (-0.95 V) are much lower than those of malathion (0.6 V) and monocrotophos (0.87 V) [37-42]. The decreasing values of $k_q^{av}$with the increasing E_{ox}indicate that the process of PL quenching is also governed by the hole transfer process from the photoexcited NMOF**1** to the OPs. Therefore, it can be proposed that the selectivity in the PL quenching by the tested OPs may also depend upon their redox potentials and presence of electron withdrawing group. The involved donor–acceptor electron-transfer is obviously dominant in presence of $–NO_2$ aromatic compounds. Therefore we can say that stronger quenching effect due to the presence of strong electron withdrawing nitroaromatic compounds on OPs offer on-off response for the proposed optical sensors**.**

Conclusions. The synthesis of luminescent NMOF**1** is presented and the product has been exploited for the sensitive sensing of $-NO_2$ aromatic OPs namely, parathion, methyl parathion, paraoxon and fenitrothion. The formation of NMOF**1** particles has been verified with different analytical techniques. The PL of the dispersed NMOF**1** results from the photoinduced intra-ligand electron transfer from. The presence of $–NO_2$ aromatic OPs is detected through the PL quenching due to strong electron withdrawing group and donor–acceptor electron-transfer mechanism, which, in turn, is also related to the oxidation potentials of the pesticides. The linear range of detection is 5 ppb - 600 ppb with detection limit of the proposed method being 5 ppb. The above data remain valid for the mixture of $–NO_2$/OPs. The proposed method was also investigated for other OPs, e.g. malathion,

dichlorvos and monocrotophos which make more selective due to absence of strong electron withdrawing group. Finally, the $–NO_2$ aromatic OPs exhibited stronger quenching effect which can be attributed to the strong electron withdrawing group which work as on-off response for the proposed optical sensor.

In addition, this type of utility of luminescent NMOF**1** has offered the label-free and direct chemosensing of the $–NO_2$ aromatic OPs. The NMOF**1** have great potential in the solid-phase extraction and enrichment of the pesticide residues also. We are continuing our investigations towards the simultaneous enrichment and quantitative detection of pesticides using luminescent NMOFs so as to obtain ultra-sensitive and label-free quantifications. The regeneration of NMOF**1** PL is also a part of the on-going / future research.

Funding Sources

The reported work has been funded through CSIR, India grant (OMEGA/PSC0202/2.2.5) from CSIR, India. One of the authors (Pawan Kumar) also acknowledges CSIR for his Senior Research Fellowship**.**

ACKNOWLEDGEMENTS

Authors thank Mr. Parveen Kumar & Vasudha Bansal for his help in conducting the experimental works. We are also grateful to the Director, CSIR-CSIO, Chandigarh for providing facilities.

Reference

1. Eddleston, M.; Buckley, N. A.; Eyer, P.; Dawson, A. H. Management of acute organophosphorus pesticide poisoning. The Lancet 2008, 371 (9612), 597.
2. Soltaninejad, K.; Abdollahi, M. Current opinion on the science of organophosphate pesticides and toxic stress: a systematic review. Medical

science monitor : international medical journal of experimental and clinical research 2009, 15 (3), RA75.
3. Bassi, A. S.; Flickinger, M. C., Biosensors, Environmental. In Encyclopedia of Industrial Biotechnology, John Wiley & Sons, Inc.: 2009.
4. Smith, A. G.; Gangolli, S. D. Organochlorine chemicals in seafood: occurrence and health concerns. Food and Chemical Toxicology 2002, 40 (6), 767.
5. Knapton, D.; Burnworth, M.; Rowan, S. J.; Weder, C. Fluorescent Organometallic Sensors for the Detection of Chemical-Warfare-Agent Mimics. Angewandte Chemie International Edition 2006, 45 (35), 5825.
6. Zourob, M.; Ong, K. G.; Zeng, K.; Mouffouk, F.; Grimes, C. A. A wireless magnetoelastic biosensor for the direct detection of organophosphorus pesticides. Analyst 2007, 132 (4), 338.
7. Zhao, X.; Hwang, H.-M. A Study of the Degradation of Organophosphorus Pesticides in River Waters and the Identification of Their Degradation Products by Chromatography Coupled with Mass Spectrometry. Arch Environ Contam Toxicol 2009, 56 (4), 646.
8. Hu, S.-Q.; Xie, J.-W.; Xu, Q.-H.; Rong, K.-T.; Shen, G.-L.; Yu, R.-Q. A label-free electrochemical immunosensor based on gold nanoparticles for detection of paraoxon. Talanta 2003**,** 61 (6), 769.
9. Amaya-Chávez, A.; Martínez-Tabche, L.; López-López, E.; Galar-Martínez, M. Methyl parathion toxicity to and removal efficiency by Typha latifolia in water and artificial sediments. Chemosphere 2006, 63 (7), 1124.
10. Kojima, H.; Takeuchi, S.; Nagai, T. Endocrine-disrupting Potential of Pesticides via Nuclear Receptors and Aryl Hydrocarbon Receptor. Journal of Health Science 2010, 56 (4), 374.
11. kazemi, m.; Tahmasbi, A. M.; VALIZADEH, R.; Naserian, A. A. Organophosphate pesticides: A general review. Agricultural Science Research Journals 2012.
12. Kwong, T. C. Organophosphate Pesticides: Biochemistry and Clinical Toxicology. Therapeutic Drug Monitoring 2002, 24 (1), 144.
13. Mulchandani, A.; Chen, W.; Mulchandani, P.; Wang, J.; Rogers, K. R. Biosensors for direc determination of organophosphate pesticides. Biosensors and Bioelectronics 2001, 16 (4–5), 225.
14. Jaffrezic-Renault, N. New Trends in Biosensors for Organophosphorus Pesticides. Sensors 2001, 1 (2), 60.
15. Liu, G.; Song, D.; Chen, F. Towards the fabrication of a label-free amperometric immunosensor using SWNTs for direct detection of paraoxon. Talanta 2013, 104 (0), 103.
16. Gong, J.; Miao, X.; Zhou, T.; Zhang, L. An enzymeless organophosphate pesticide sensor using Au nanoparticle-decorated graphene hybrid nanosheet as solid-phase extraction. Talanta 2011, 85 (3), 1344.
17. Gong, J.; Miao, X.; Wan, H.; Song, D. Facile synthesis of zirconia nanoparticles-decorated graphene hybrid nanosheets for an enzymeless methyl parathion sensor. Sensors and Actuators B: Chemical 2012, 162 (1), 341.
18. Kanagaraj, K.; Affrose, A.; Sivakolunthu, S.; Pitchumani, K. Highly selective fluorescent sensing of fenitrothion using per-6-amino-β-cyclodextrin:Eu(III) complex. Biosensors and Bioelectronics 2012, 35 (1), 452.
19. M. D. Allendorf , C. A. Bauer , R. K. Bhakta and R. J. T. Houk Luminescent metal–organic frameworks Chem. Soc. Rev.**,** 2009**,**38**,** 1330-1352.

20. Alexander U. Czaja, Natalia Trukhan and Ulrich Müller, Industrial applications of metal organic frameworks, Chem. Soc. Rev., 2009, 38, 1284-1293.
21. Guan-Yao Wang, Chan Song, De-Ming Kong, Wen-Juan Ruan, Ze Chang and Yue Li, Two luminescent metal–organic frameworks for the sensing of nitroaromatic explosives and DNA strands, J. Mater. Chem. A**,** 2014**,** 2**,** 2213-2220.
22. Lan, A.; Li, K.; Wu, H.; Olson, D. H.; Emge, T. J.; Ki, W.; Hong, M.; Li, J. A Luminescent Microporous Metal–Organic Framework for the Fast and Reversible Detection of High Explosives. Angewandte Chemie International Edition 2009, 48 (13), 2334.
23. P. Kumar, A. Deep, A. K. Paul L. M. Bharadwaj, Bioconjugation of MOF-5 for molecular sensing, J Porous Mater 21 (2014) 99–104.
24. Pawan Kumar, Parveen Kumar, Lalit M. Bharadwaj, A.K. Paul, Akash Deep, Luminescent nanocrystal metal organic framework based biosensor for molecular recognition, Inorganic Chemistry Communications 43 (2014) 43, 114–117.
25. McKinlay AC, Morris RE, Horcajada P, Férey G, Gref R, Couvreur P, Serre C. Bio MOFs: Metal – Organic Frameworks for Biological and Medical Applications, Angrew Chem. 49 (2010) 6260-6266.
26. K.K. Tanabe, S.M. Cohen, Postsynthetic modification of metal–organic frameworks: a progress report, Chem. Soc. Rev. 40 (2011) 498–519.
27. Y.B. Zhang, W.X. Zhang, F.Y. Feng, J.P. Zhang, X.M. Chen, A highly connected porous coordination polymer with unusual channel structure and sorption properties, Angew. Chem. Int. Ed. 48 (2009) 5287–5290.
28. Kreno, L. E.; Leong, K.; Farha, O. K.; Allendorf, M.; Van Duyne, R. P.; Hupp, J. T. Metal–organic framework materials as chemical sensors. Chemical Reviews 112 (2) (2011) 1105.
29. C. Wang, Z. Xie, K.E. deKrafft, W. Lin, Doping metal–organic frameworks for water oxidation, carbon dioxide reduction, and organic photocatalysis, J. Am. Chem. Soc.133 (2011) 13445–13454.
30. Wen, L.-L.; Wang, F.; Leng, X.-K.; Wang, C.-G.; Wang, L.-Y.; Gong, J.-M.; Li, D.-F. Efficient Detection of Organophosphate Pesticide Based on a Metal−Organic Framework Derived from Biphenyltetracarboxylic Acid. Crystal Growth & Design 10 (7), (2010) 2835.
31. F. Wang, X. Ke, J. Zhao, K. Deng, X. Leng, Z. Tian, L. Wen, D. Li, Six new metal– organic frameworks with multi-carboxylic acids and imidazole-based spacers:syntheses, structures and properties, Dalton Trans. 40 (2011) 11856–11865.
32. Yun-Peng Wang , Feng Wang , Ding-Feng Luo, Li Zhou, Li-Li Wen A luminescent nanocrystal metal–organic framework for sensing of nitroaromatic compounds ,Inorganic Chemistry Communications 19 (2012) 43–46.
33. S. Pramanik, C. Zheng, X. Zhang, T.J. Emge, J. Li, New microporous metal–organic framework demonstrating unique selectivity for detection of high explosives and aromatic compounds, J. Am. Chem. Soc. 133 (2011) 4153–4155.
34. B.L. Chen, L.B. Wang, Y.Q. Xiao, F.R. Fronczek, M. Xue, Y.J. Cui, G.D. Qian, A luminescent metal–organic framework with lewis basic pyridyl sites for the sensing of metal ions, Angew. Chem. Int. Ed. 48 (2009) 500–503.

35. D. Tanaka, A. Henke, K. Albrecht, M. Moeller, K. Nakagawa, S. Kitagawa, J. Groll, Rapid preparation of flexible porous coordination polymer nanocrystals with accelerated guest adsorption kinetics, Nat. Chem. 2 (2010) 410–416.
36. W. Cho, H.J. Lee, M. Oh, Growth-controlled formation of porous coordination polymer particles, J. Am. Chem. Soc. 130 (2008) 16943–16946.
37. ZHANG Lu, Z. Y.-d., QI Hong-lan Determination of Malathion Based on Carbon Nanotubes Modified Electrode Incorporating Acetylcholinesterase. Journal of Electrochemistry 2007, 13 (04), 431.
38. A.J. Lan, K.H. Li, H.H. Wu, D.H. Olson, T.J. Emge, W. Ki, M.C. Hong, J. Li, A luminescent microporous metal–organic framework for the fast and reversible detection of high explosives, Angew. Chem. Int. Ed. 48 (2009) 2334–2338.
39. Suhyun Jung, Youngmee Kim, Sung-Jin Kim, Tae-Hwan Kwon, Seong Huh and Seongsoon Park, Bio-functionalization of metal–organic frameworks by covalent protein conjugation. Chem. Commun. 47**(**2011) 2904-2906.
40. D.Y. Ma, W.X. Wang, Y.W. Li, J. Li, C. Daiguebonne, G. Calvez, O. Guillou, In situ 2,5-pyrazinedicarboxylate and oxalate ligands synthesis leading to a microporous europium-organic framework capable of selective sensing of small molecules, CrystEngComm 12 (2010) 4372–4377.
41. Liu, G.; Lin, Y. Electrochemical stripping analysis of organophosphate pesticides and nerve agents. Electrochemistry Communications 2005, 7 (4), 339.
42. Hu, S.-Q.; Xie, J.-W.; Xu, Q.-H.; Rong, K.-T.; Shen, G.-L.; Yu, R.-Q. A label-free electrochemical immunosensor based on gold nanoparticles for detection of paraoxon. Talanta 2003, 61 (6), 769.

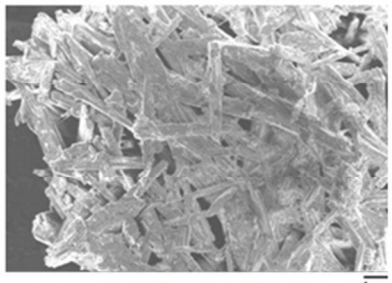

FE-SEM images of NMOF1

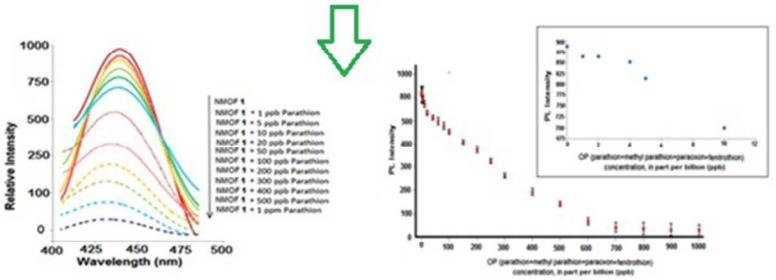

Effect of the addition of different concentrations of Parathion on the PL intensity of NMOF1. Separately investigated, other nitro OPs (methyl parathion, paraoxon, fenitrothion) also yielded similar pattern of PL quenching.

Effect of the addition of different concentrations of mixed $-NO_2$ OPs mixture on the PL intensity of NMOF1 (Inset image reveals the measurements at low concentrations).

186x141mm (96 x 96 DPI)

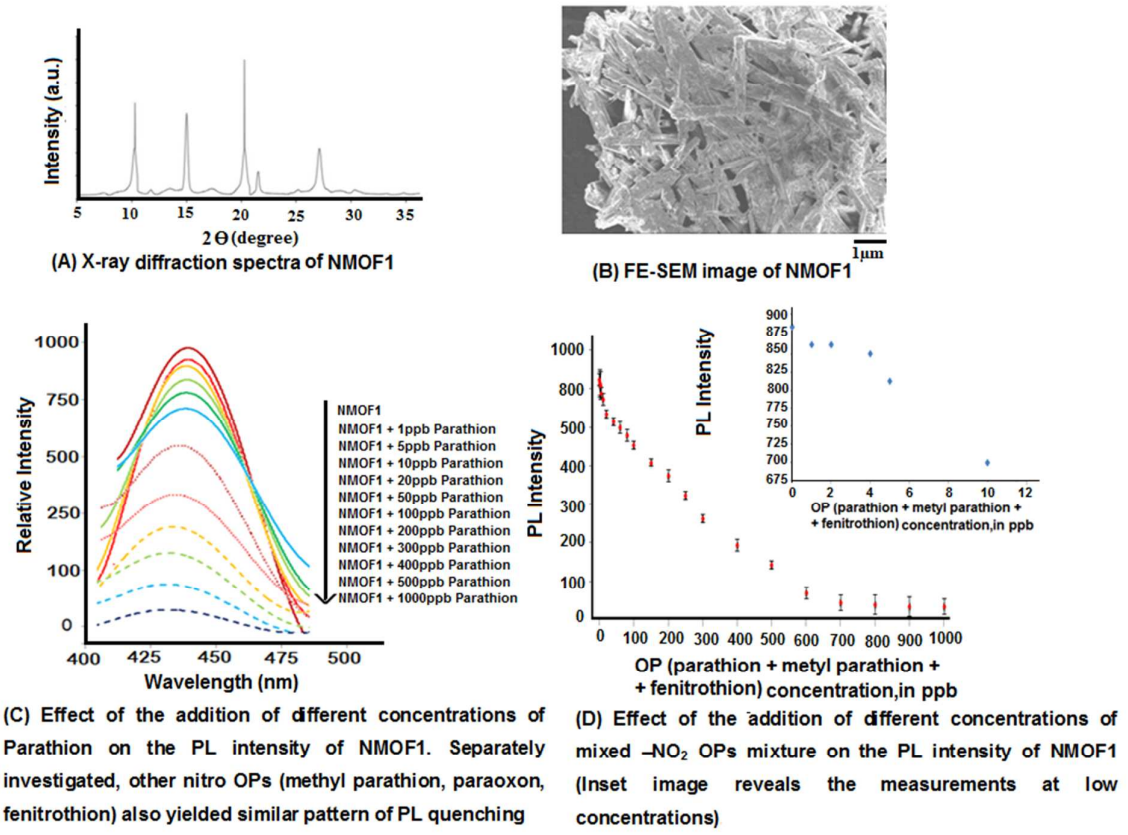

Fig.1. (A): (I) X-ray diffraction spectra of synthesized NMOF1 & correlated with reference X-ray diffraction spectra of NMOF1, **(B)** FE-SEM images of NMOF1, **(C)** Effect of the addition of different concentrations of Parathion on the PL intensity of NMOF1. Separately investigated, other nitro OPs (methyl parathion, paraoxon, fenitrothion) also yielded similar pattern of PL quenching and **(D)** Effect of the addition of different concentrations of mixed –NO_2 OPs mixture on the PL intensity of NMOF1 (Inset image reveals the measurements at low concentrations).

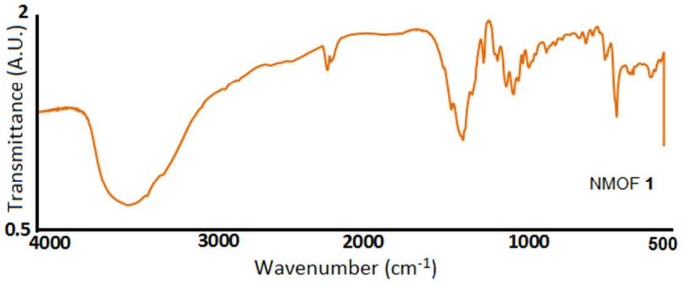

Fig. 2. FTIR spectra of NMOF**1**.

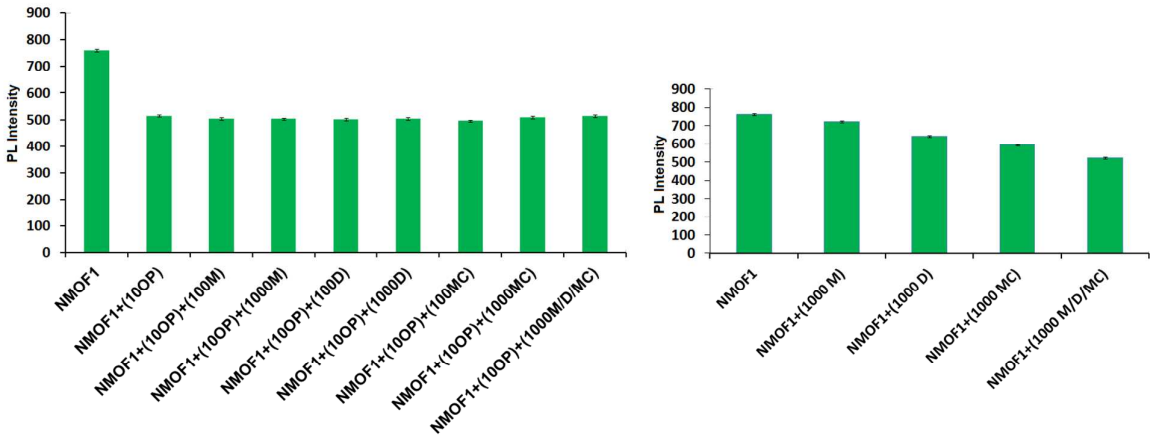

Fig. 3 (A) Selectivity of PL quenching by $-NO_2$ OPs in the presence of other OPs (OP= $-NO_2$ OPs; M = malathion, D = dichlorvos; MC = monocrotophos; 10 = 10 ppb; 100 = 100 ppb, 1000 = 1000 ppb) and **(B)** Effect on the PL intensity of NMOF**1** in the presence of malathion (M), dichlorvos (D) and monocrotophos (MC); 1000 = 1000 ppb, (ppb = part per billion).

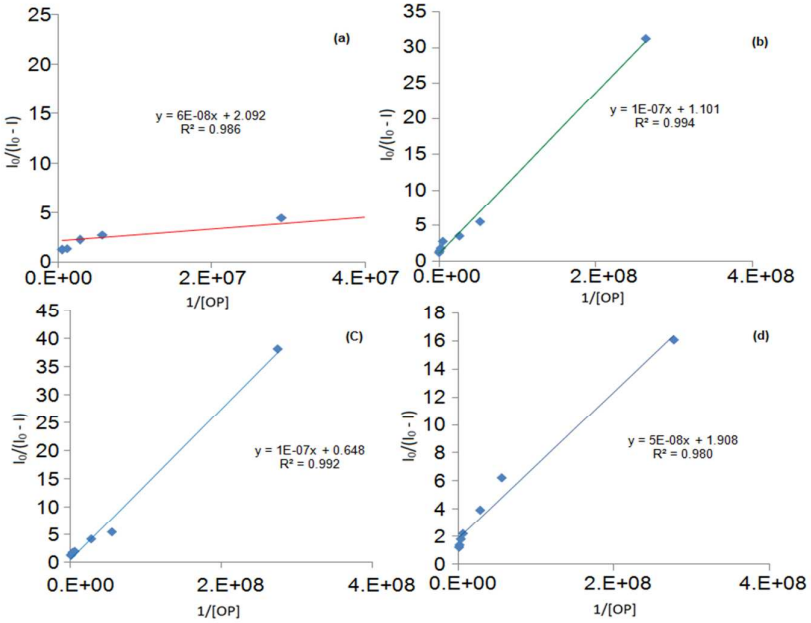

Fig.4.Stern – Volmer (reciprocal) plot for the PL quenching experiments with parathion (a); methyl parathion (b); paraoxon (c); fenitrothion (d), [OP] concentration unit is in mol/L.

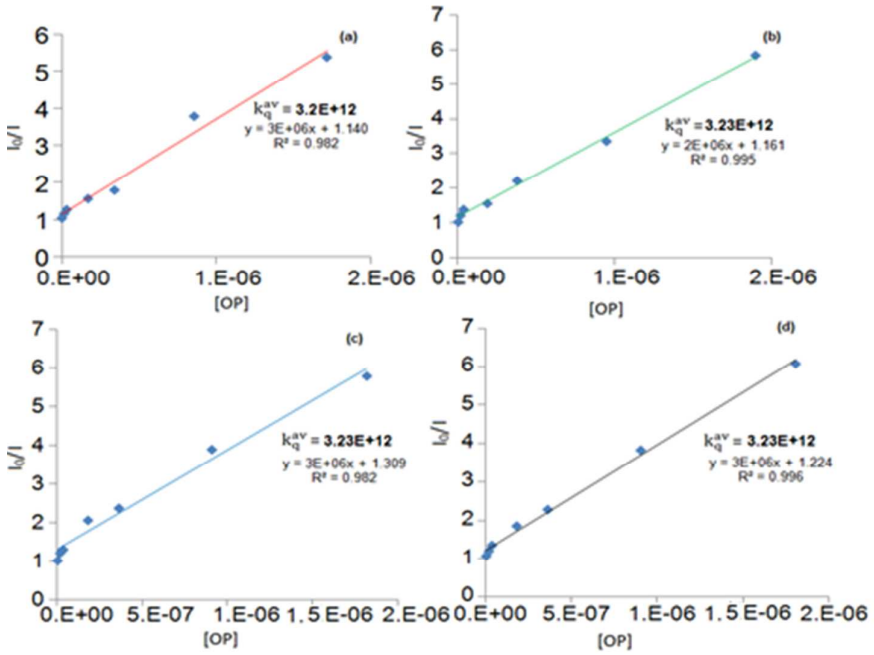

Fig.5. Stern – Volmer plot for the PL quenching experiments with parathion (a); methyl parathion (b); paraoxon (c); fenitrothion (d), [OP] concentration unit is in mol/L.

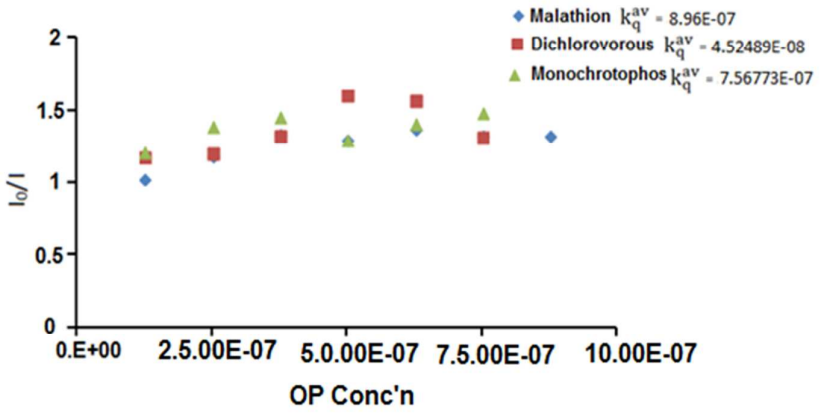

Fig.6. Stern – Volmer plot for the PL quenching experiments with malathion, dichlorvos and monocrotophos, [OP] concentration unit is in mol/L.